

PLASTIC DEFORMATION OF B.C.C. POLYCRYSTALS : COMPARISON BETWEEN EXPERIMENTAL DATAS AND RESULTS OF SEVERAL MODELLING CODES.

F. ROYER⁽¹⁾, A. NADARI⁽²⁾, F. YALA⁽³⁾, P. LIPINSKI⁽²⁾
D. CECCALDI⁽³⁾, M. BERVEILLER⁽²⁾, P. PENELLE⁽³⁾.

(1) Université de METZ, IPER, CMSR/LPMC, 1 boulevard Arago, 57070 METZ.

(2) Université de METZ, LPMM/ISGMP, Ile du Saulcy, 57045 METZ Cedex 01.

(3) Laboratoire de Métallurgie Structurale, UA1107, bat.413, 91405 ORSAY.

This contribution complete a previous one (1) in that the specific problems of the elastoplastic behaviour of body-centered polycrystals are analyzed. The experimental results (yield stress, Lankford's ratio, textures, ...) are compared with those of self-consistent and Taylor modelling codes. A particular attention is put on the influence of the selection of glide systems in the framework of crystallographic or non-crystallographic assumptions.

1) PRESENTATION OF THE EXPERIMENTAL DATA.

The sample which is studied is a low carbon rimmed steel. The initial state is a recrystallized sheet (thickness = 0.7mm) with equiaxed grains (mean diameter=20 μ m). Table 1 summarizes some mechanical properties such as the lower and upper value of the yield stress (because of the existence of a yield point), the ultimate tensile stress (R_m) and strain failure (A_m).

In addition table 2 contains the experimental measurements of the Lankford's ratio obtained respectively with a coincidence rule and from a deposit of 1mmx1mm grids (IRSID license).

The mean value \bar{R} appears low and it can be concluded that the mechanical properties of the retained material are not very anisotropic.

On an other hand, the (110), (200) and (112) poles figures have been measured by a classical X-rays reflexion method and completed by an original extrapolation developed by Baudin et al. (2)

Figure 1 shows the poles figures of the initial state. The existence of an orthotropic symmetry nearby a fiber around the normal direction and the <110> orientation can be pointed out.

Finally by taken in account the informations of the orientation distribution function the initial state of the studied material is described by a $(111)\langle uvw \rangle$ fiber associated with a secondary component $(100)\langle 110 \rangle$.

TABLE 1 Mechanical properties : R_e (yield stress), R_m (ultimate tensile stress), A_m (ultimate strain failure) vs angle to the rolling direction.

α vs RD (°)	yield stress lower bound	R_e (MPA) upper bound	R_m (MPA)	A_m (%)
0	191	206	401	24
15	191	209	407	24
30	194	210	414	24
45	194	215	413	24
60	193	215	415	24
75	190	208	406	24
90	191	207	402	24

TABLE 2 Lankford's ratio : (1) coincidence rule, (2) grids.

α (°)	0	15	30	45	60	75	90	\bar{R}	ΔR
$R(\alpha)$ [1]	1.78	1.69	1.54	1.36	1.61	1.97	1.09	1.64	0.57
$R(\alpha)$ [2]	1.97	1.84	1.68	1.36	1.90	1.96	2.11	1.70	0.68

2°) EVOLUTION OF THE EXPERIMENTAL DEFORMATION TEXTURES.

A tensile test is performed successively along, parallel to and at 45° of the rolling direction.

a) Tensile test along the rolling direction.

At a 20% deformation stage a reinforcement of the (110) poles density is observed. Simultaneously the fiber texture vanishes. The $(111)\langle 110 \rangle$ component is always present and the density increases whereas the $(111)\langle 112 \rangle$ component decreases. Globally a deformation along RD leads to a reinforcement of the texture. This conclusion is illustrated by figure 2a-b.

b) If the uniaxial deformation is imposed this time along the transverse direction, a rotation of 30° around the normal direction is observed but the orthotropic symmetry is conserved (figure 3a). The $(111)\langle 110 \rangle$ component decreases, $(111)\langle 112 \rangle$ increases and $(100)\langle 110 \rangle$ stays at low values.

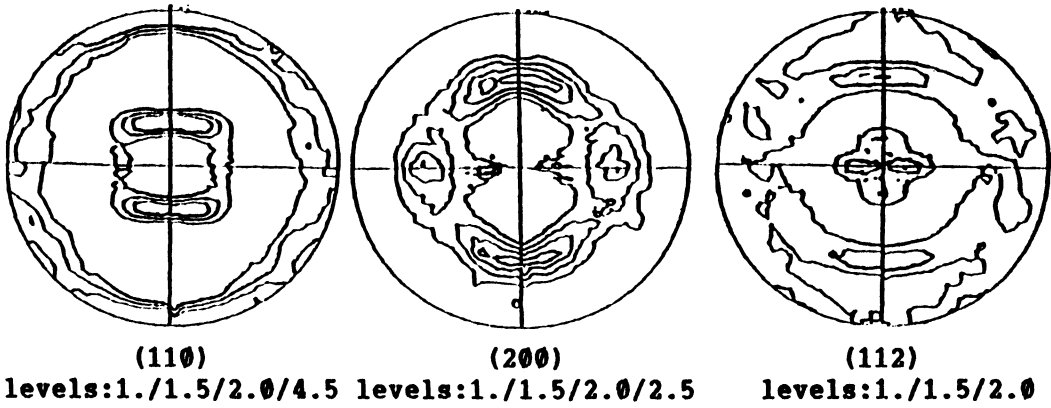


figure 1 : poles figures of the initial state

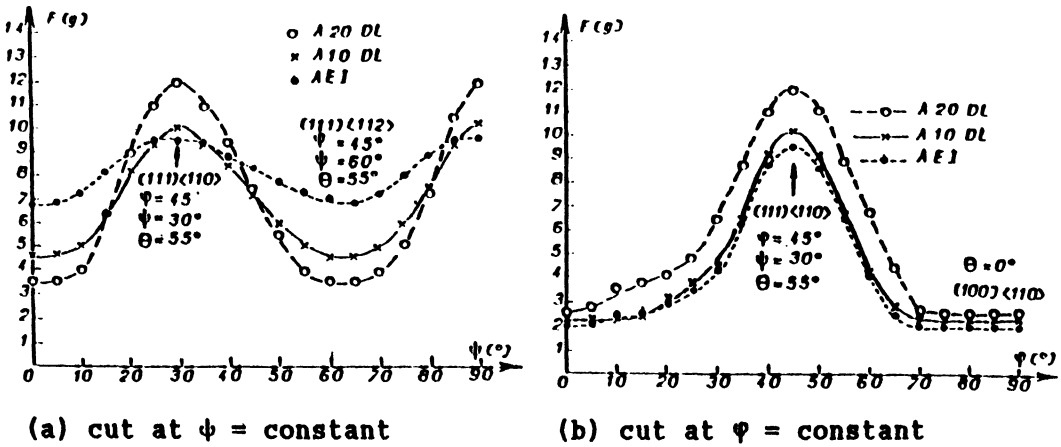


figure 2 : variations of the ODF.

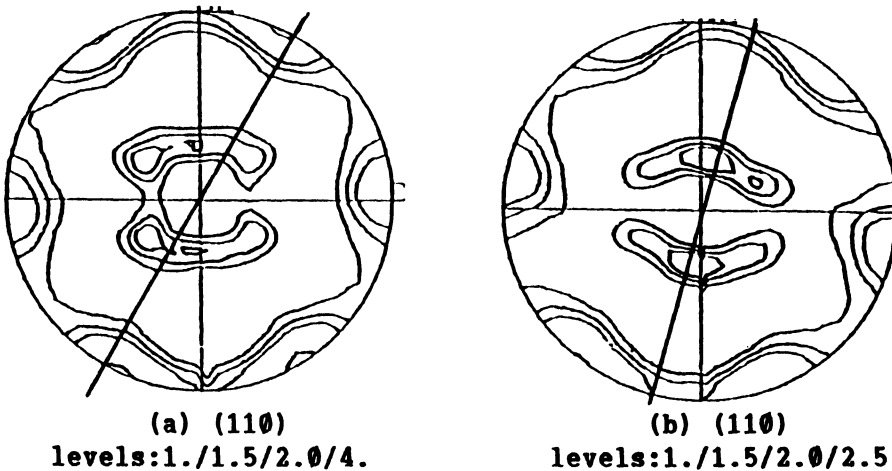


figure 3: poles figures (a) tensile test // TD - rotation 30° around ND, (b) tensile test 45° of RD - rotation 15° around ND.

c) At last, to fulfill observations on eventual deformation heterogeneities the mechanical test is performed out of the main axes (45° vs RD) with fixed grips. All the poles figures present a rotation of 15° around the normal direction with loss of the initial symmetry (figure 3b). This last point can be confirmed by the representative curve of the skeleton drawn at $\varphi = \text{constant}$. The loss of the symmetry is characterized by the splitting of the $(hkl)\langle uvw \rangle$ components which are no more equivalent (figure 4).

3') APPLICATIONS OF THE MODELLING CODES.

Even though the glide directions are well determined as $\langle 111 \rangle$ directions, the slip planes can belong to the $\{110\}$, $\{112\}$ or $\{123\}$ families.

The elastoplastic behaviour of bcc polycrystals will be described in this communication by two set of modelling codes:

a) Taylor type models:

- the classical Taylor model (3) based on a crystallographic assumption leads to the activation of 6 or 8 systems between the 12 possible $\{110\}\langle 111 \rangle$ systems;

- in an other way, it is feasible to introduce a mixed assumption. The glide systems are that time chosen between the two $\{110\}\langle 111 \rangle$ and $\{112\}\langle 111 \rangle$ sets. Compared to the previous works (4,5) an original computational scheme has been developed by Ceccaldi and al. (6) based on the 15 irreducible groups of vertices deduced from the critical Bishop-Hill polyhedron (7). To each group is associated a combinaison of 5,6 or 8 active slip systems;

- from an experimental point of view the two models which precede tend to activate a too higher number of systems. So an usual assumption for bcc materials is to retain only the glide systems which verify a maximal shear stress criteria (4 or 5 systems are activated) (8).

b) A self consistent approach developed by Berveiller and al. (9).

An one site model based on an ellipsoidal inclusion in an anisotropic matrix with tangential elastoplastic behaviour is used. The glide systems are indifferently chosen between the 24 $\{110\}\langle 111 \rangle$ or 48 ($\{110\}\langle 111 \rangle + \{112\}\langle 111 \rangle$) systems. At the first step of the calculations the critical shear stress is the same on all the systems. The grain shape is set on the equiaxed one. The hardening matrix contains two types of values (H_2, H_1 with $H_2 = AH_1$) with an anisotropic factor $A = 1.1$. A minimal set of 100 grains is put out of the experimental measurements of the poles figure.

4') RESULTS AND DISCUSSION.

- Figure 5 shows the behaviour of the Lankford's ratio $R(\alpha)$. The mixed combination $\{110\}\langle 111 \rangle + \{112\}\langle 111 \rangle$ gives a very

good agreement with the experimental data still better than the so-called pencil glide model. The crystallographic glide limited to the $\{110\}\langle 111 \rangle$ appears largely non-realistic for bcc polycrystals;

- figure 6 presents the comparison of the experimental and calculated ODF by the way of a cut at $\psi = 45^\circ$. The peaks are well placed even the intensities are higher on the calculated figure.

- Figure 7 illustrates the experimental and calculated (200) poles figures at 45° from the rolling direction for a 20% deformation and activation only of the $\{110\}\langle 111 \rangle$ systems. The theoretical calculations reproduce correctly the rotation of 15° around the normal direction and give a good agreement with the most important peaks. Introducing the complete set of forty-eight $\{110\}\langle 111 \rangle + \{112\}\langle 111 \rangle$ systems does not allow significant changes.

5) CONCLUSION.

The fundamental assumption of the modelling codes used in this contribution is that the local deformation mechanism is manifold homogeneous glide. The Taylor type models lead to several results in good agreement with the experience according to the assumptions included in the theory. Concerning the self consistent model between all the results obtained it can be noticed the low influence of the geometrical parameters such as the grain shape, number of glide systems and anisotropy factor (introduced in the hardening matrix).

REFERENCES.

- (1) F. Royer, T. Baudin, D. Ceccaldi, R. Penelle, C. Peyrac and C. Vial, this conference.
- (2) T. Baudin, R. Penelle, D. Ceccaldi, F. Royer, Mem. Et. Sci. Rev. Metallurgie, 10, 611 (1990)
- (3) G.I. Taylor, J. Inst. Metals, 62, 307 (1938)
- (4) P. van Houtte and E. Aernoudt, Mat. Sci. Eng., 23, 11 (1976)
- (5) P. van Houtte, Acta Met., 26, 591 (1978)
- (6) D. Ceccaldi, T. Baudin, R. Penelle, F. Royer, to be published
- (7) B. Orleans-Joliet, B. Bacroix, F. Montheillet, J. Driver and J.J. Jonas, Acta Met., 36, 1365 (1988)
- (8) F. Royer, C. Tavard and P. Penning, J. Appl. Cryst., 12, 436 (1979)
- (9) P. Lipinski and M. Berveiller, Int. J. Plasticity, 5, 149 (1989)

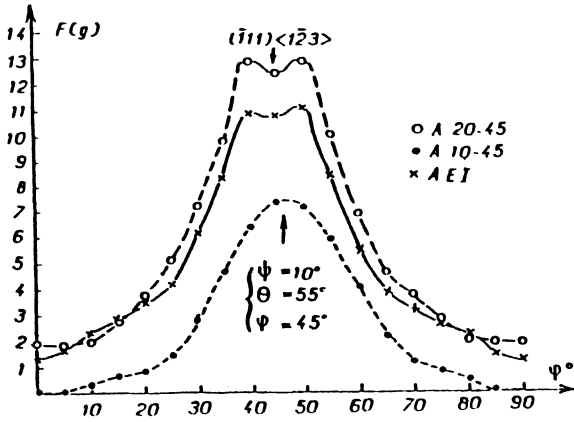


figure 4:ODF squeleton (ψ =constant) splitting of the $(hkl)\langle uvw \rangle$ orientations

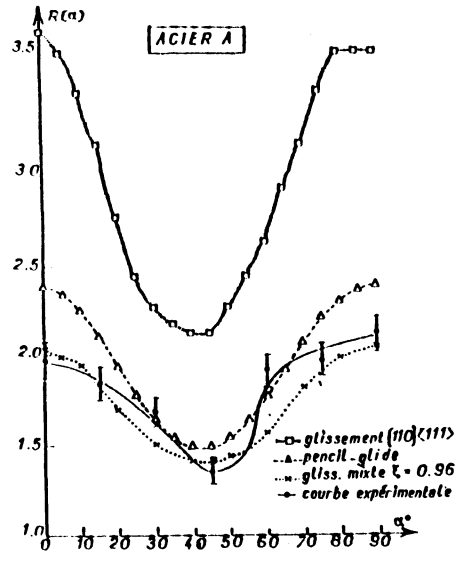


figure 5:Lankford's ratio for Taylor's type models

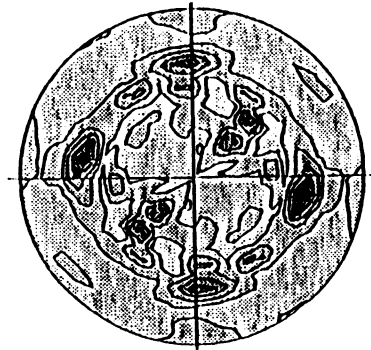
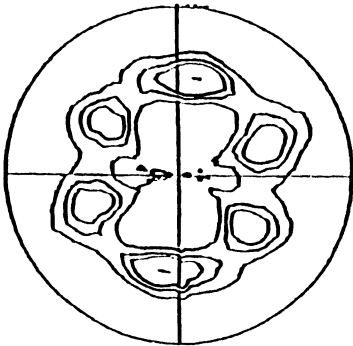


figure 6:(200) pole figure (a)experience (b)self consistent code.

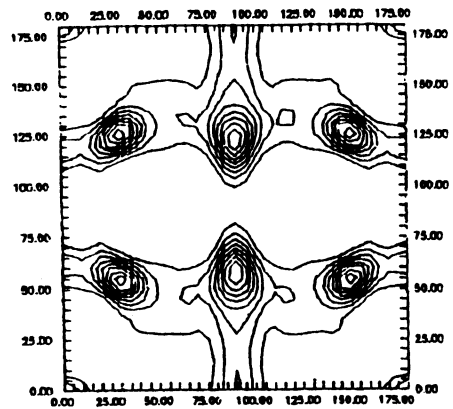
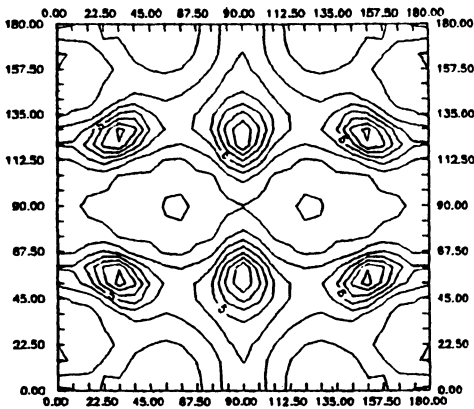


figure 7 : cut at 45° - 20% deformation along RD (a) experience (b) mixed slip systems